CHALMERS
UNIVERSITY OF TECHNOLOGY

Ultra-Wideband 90 degrees Waveguide Twist for THz applications

Citation for the original published paper (version of record):
López, C., Montofre, D., Desmaris, V. et al (2023). Ultra-Wideband 90 degrees Waveguide Twist for THz applications. IEEE Transactions on Terahertz Science and Technology, 13(1): 67-73.
http://dx.doi.org/10.1109/TTHZ.2022.3213468

(article starts on next page)

T-TST-REG-06-2022-00102.R1

Ultra-Wideband 90º Waveguide Twist for THz applications

C. D. López, D. Montofré, V. Desmaris, A. Henkel and V. Belitsky, *Senior Member*, IEEE

***Abstract*— We report on the design, fabrication, and characterization of a novel 90º waveguide step twist with 56% fractional bandwidth. The proposed twist provides 90º field rotation in the frequency range 210-375 GHz. The experimental results are in good agreement with the electromagnetic simulations showing an insertion loss below 0.3 dB and a return loss better than 20 dB over most of the band. The ultra-wideband performance, tolerance to fabrication inaccuracies and compactness makes the proposed design attractive for various mm and sub-millimeter applications. The twist geometry is optimized for simple fabrication through direct milling. Furthermore, the design remains highly compact since both steps are fabricated on a single washer.**

***Index Terms*— 90º twist, Waveguide twist, THz applications, millimeter/submillimeter wave, astronomical applications, space applications.**

I. Introduction

THE development of ultra-wideband components at mm and sub-mm frequencies is crucial for applications in multiple research fields, e.g. radio astronomy [1-5], biomedical science [6], and material science [7]. Moreover, modern communications systems such as the fifth-generation wireless communication (5G) have made extensive use of broadband millimeter-wave (mm-wave) components [8]. In addition, the future sixth-generation wireless communication system (6G) is expected to make use of higher frequency bands beyond the mm-wave up to THz bands [8], [9]. On the other hand, radio astronomy science goals for the next decades require the development of components with high fractional bandwidth and state of the art performance [12]. In particular, dual-polarization heterodyne receivers [3-5], [11-13] will be key for astronomical observations at THz frequencies, e.g. the event horizon of a supermassive black hole, and the red super-giant VY Canis Majoris [14].

THz heterodyne receivers with dual-polarization detection frequently rely on orthomode transducers (OMTs) [5]. Since the OMT outputs are generally orthogonal to each other, the E field of one of the output waveguides often needs to be rotated 90º to facilitate the integration of the two signal chains into a single receiver system. Electromagnetic field rotation is frequently achieved by employing a waveguide twist. Therefore, waveguide twists have become an essential component for receivers with polarization discrimination. Numerous designs for waveguide twists have been investigated throughout the years. For instance, a classical solution is found in continuous twists. Such twists provide broadband performance with excellent matching over the whole bandwidth. This type of twist is traditionally produced by gradually twisting a rectangular waveguide along its longitudinal axis [15]. Alternatively, they could be fabricated with an aluminum mold and electroforming to achieve better geometric accuracy. However, these fabrication methods are complex and expensive. Furthermore, continuous twists are difficult to implement in systems where compactness is a major concern, e.g., space-borne applications where the weight and size of the payload must be minimized without degrading the overall system performance [16], [12]. Moreover, continuous twists are long waveguide components that introduce losses that are significant at frequencies above 100 GHz, and consequently, they could degrade the performance of, e.g., a receiver.

An alternative solution was explored in the designs presented in [17], [18], which are based on multi-step twists. These twists are formed by a series of waveguide sections that are gradually rotated until the full E-field rotation is achieved. Although this solution is less bulky than a continuous twist, the overall performance of the multi-step twists depends on the fabrication and mounting tolerances of each section. Therefore, these twists are especially challenging to implement at higher frequencies where mounting tolerances are more critical.

The 90° single-step twists constitute the most compact solution [19-23]. In this approach, a single section is inserted in the waveguide system with an angle of 45°, which allows the E-field to rotate. Nonetheless, it remains rather difficult to achieve fractional bandwidth larger than 44% with single step-twists [22].

In this work, we present a novel 90º twist that combines a tolerant geometry, compactness, and ultra-broadband performance with 56% fractional bandwidth at THz frequencies. Moreover, the suggested geometry can be realized by direct milling of two twist sections on a single washer. This configuration considerably eases the fabrication and eliminates the mounting inaccuracy between the sections.

The proposed design is intended to cover the frequency band 210-375GHz. This frequency range was selected since it

C. D. López, D. Montofré, V.Desmaris and V.Belitsky are with the Group for Advance Receiver Development (GARD), Chalmers University of Technology, Gothenburg, Sweden. (e-mail: cristian.lopez@chalmser.se). A. Henkel is with the Rohde & Schwarz GmbH & Co. KG, Munich, 81671, Germany.

This article has been accepted for publication in IEEE Transactions on Terahertz Science and Technology. This is the author's version which has not been fully edited and content may change prior to final publication. Citation information: DOI 10.1109/TTHZ.2022.3213468

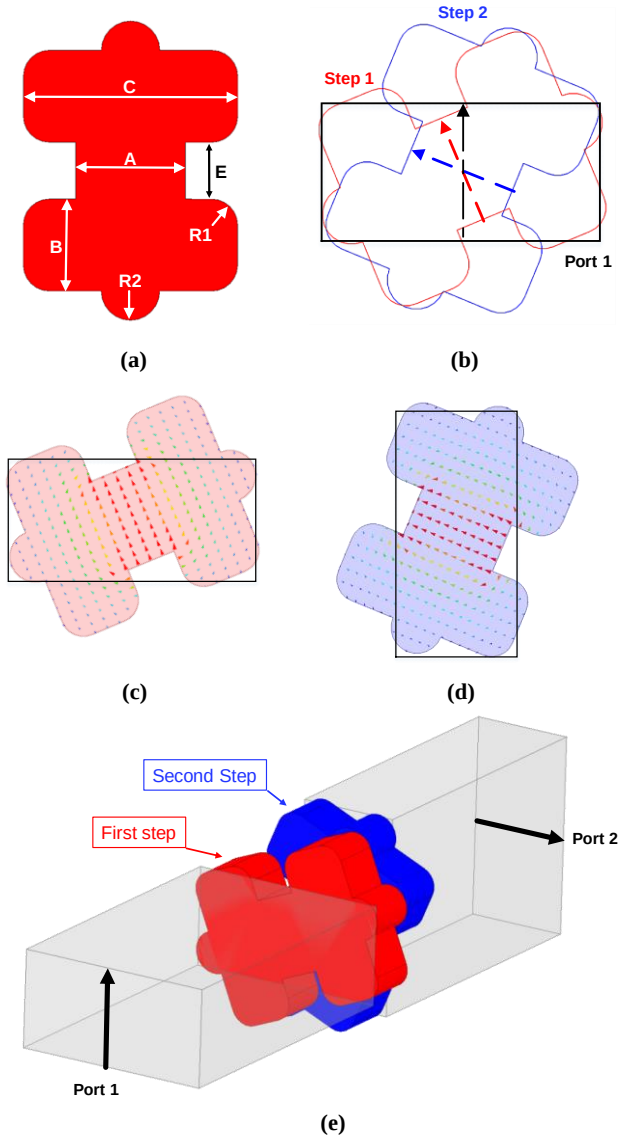

Fig. 1. Proposed waveguide twist. (a) The twist configuration consists of two adjacent and identical steps milled on opposite sides of a single washer. The designed values are: A=318 µm, B=267 µm, C=622 µm, E= 166 µm, R1=75 µm, and R2= 85 µm. The thickness of each step is 210 µm. (b) Rotation of the electric field corresponding to the main propagation mode. The orientation of the electric field is depicted in red for the first step, blue for second step and black for the rectangular waveguide (port 1). The first step allows the rotation of the field 22.5º while the second further rotates the E-field 67.5º. The angles are counterclockwise and referred to the field rotation of the electric field vector of port 1. (c) Dominant mode that propagates inside the first step of the twist. The mode resembles a TE_{10} mode in a ridge waveguide (d) Dominant mode that propagates inside the second step of the twist. (e) Proposed waveguide twist connected to rectangular waveguide ports. The rectangular waveguide size is 800 µm x 400 µm.

combines band 6 (211-275 GHz) and band 7 (275 GHz-375GHz) of the Atacama Large Millimeter/submillimeter Array (ALMA) [10]. However, the design is not limited to radio astronomy applications and it could be implemented in any system where compactness and wideband performance are required.

II. Theory and Design

A. Principle of Operation

The proposed twist is illustrated in Fig. 1. In order to achieve E-field rotation, a discontinuity is introduced into a waveguide where a desirable evanescent mode(s) is exited, i.e, these modes will exist inside the step twist cavity but they will not propagate in the rectangular waveguide. Single-step and multi-step twists take advantage of the electrical separation between such discontinuities to mutually cancel their reflections into single-mode waveguides, as studied in [19]. The introduction of a step twist creates a discontinuity that is generally inductive [19]. In the case of an ideal single-step twist, the discontinuities created with the input and output waveguides are identical. Therefore, if the thickness of the step is close to $\lambda_g/4$ both discontinuities will mutually cancel. It is important to note that λ_g is defined as the guided wavelength of the dominant mode inside the twist cavity.

In the case of multi-step twists is important to distinguish between two cases. In the first case, the cross section of the steps consists of a rotated rectangular waveguide of the same size as the input/output waveguides. Ideally, if the rotation angle is constant, the reactive discontinuities are equal and they might be mutually canceled if the thickness of each step is $\lambda_g/4$. In contrast, such discontinuities are not identical when the cross section of the steps is not a rectangular waveguide [24], i.e. the discontinuities created between the steps are different from the input and output ones. Hence, the thickness and the rotation angle of the steps must be adjusted to compensate for the reactive effect of unequal discontinuities. In other words, the optimum thickness of each section is different from $\lambda_g/4$, and/or the rotation angle might not be constant, i.e. the angular rotation of the input waveguide and the first step is not the same as between the steps. Such is the case with the proposed twist.

As depicted in Fig. 1, the proposed twist consists of two double ridge rectangular waveguides that are step-wise rotated to allow a final 90º rotation of the field. The waveguide with dimensions of 800 µm x 400 µm was employed to cover the target frequency range of 210-375 GHz. In our suggested design, electromagnetic simulations were employed to determine that the optimum thickness of each step must be close to 200 µm for the given frequency band. The rotation angle was optimized to maximize the fractional bandwidth. In Fig. 2 a simulation of the twist structure with different rotation angles is depicted. The optimum solution is found when, from the perspective of port 1, the field is rotated 22.5º by the first step of the twist, while the second step rotates the field at 67.5º. Such two-step E-field rotation eases the complete 90º field rotation at port 2, as illustrated by Fig.1c and d.

In addition, each twist section includes “lobes” on each side with a circular shape defined by a radius *R2*, Fig. 1a. This feature is introduced to enhance the device performance at the lower edge of the band and, consequently, broaden the bandwidth of the twist. To illustrate the increment in the RF bandwidth by introducing the “lobes”, Fig. 3 displays the

This article has been accepted for publication in IEEE Transactions on Terahertz Science and Technology. This is the author's version which has not been fully edited and content may change prior to final publication. Citation information: DOI 10.1109/TTHZ.2022.3213468

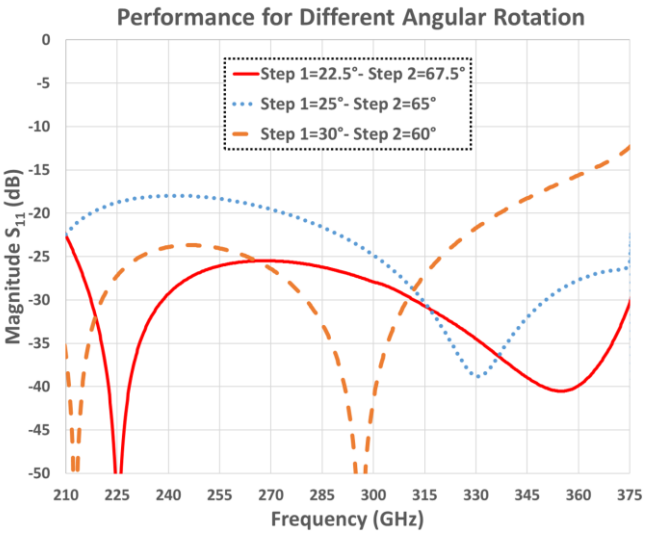

Fig. 2. Simulations of the suggested twist for different rotation angles. The rotation angles are set for step 1 and 2 as described in Fig.1. It is seen that due 22.5 º and 67.5 º maximize the fractional bandwidth of the device.

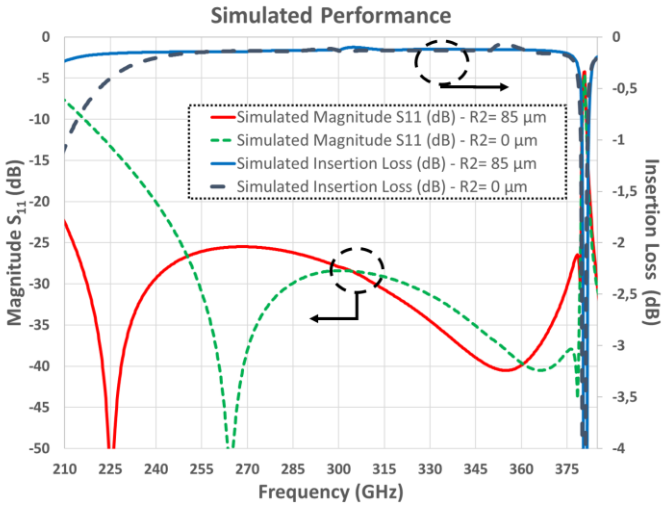

Fig. 3. Simulations of the optimized twist device. The plots show the magnitude of S11 better than 20dB over the design band and 0.25dB insertion loss. It is evident that a broader bandwidth is achieved when the circular elements are included in the twist structure.

simulated performance of the proposed twist with and without the half-circle "lobes". From the plot, it is seen that the introduction of these elements improves the performance at low frequencies. Furthermore, there is a substantial improvement in the fractional bandwidth of the twist from 45% (235-375GHz) to 56% (210-375GHz). This phenomenon could be explained by the increment in the effective width of the ridge structure. Since the lobes on each side of the structure increase the effective waveguide width, the cut-off frequency of the dominant mode decreases, and the matching is improved at the lower edge of the band. The plot in Fig. 2 also shows that a resonance appears at the higher end of the band. As investigated in [21], the resonance is related to a higher-order mode trapped inside the waveguide twist cavity. This feature imposes a clear limit on the bandwidth of the twist device at its high-frequency edge. It is important to remark that increasing B while E remains constant has a similar effect to adding the lobes. However, this introduces the resonance inside the operational bandwidth.

B. Twist Design

The starting point for the design is a double ridge waveguide that covers the target frequency range [25]. It is important to remark that the calculations presented in this section provide just an initial point for optimization. The proposed twist was designed and optimized in Ansys HFSS [26] aiming to cover the frequency range 210-375 GHz with a return loss of better than 20 dB.

The initial values of the parameters can be calculated as follows:

$$E + 2B = a_w \tag{1}$$

$$E = a_w * \alpha \tag{2}$$

$$C = a_w * \beta \tag{3}$$

where a_w is the "a" size of the input waveguide, i.e, 800 µm in the proposed design. Meanwhile, α and β affect the useful bandwidth of the device [25]. Our simulations indicate that α equal to 0.23 and β equal to 0.88 provides a reasonable starting point for the design. The remaining parameter, i.e, A, can be computed from the cut-off frequency for the dominant mode of the ridge waveguide. As an initial value, the cut-off frequency of the double ridge waveguide can be made equal to the cut-off for the dominant mode of the input rectangular waveguide. In [25], a close form for the cut-off frequency of the double ridge waveguide is detailed. For completeness, the equation is reproduced here with the parameters depicted in Fig.1 c:

$$F_C = \frac{1}{4B\sqrt{\varepsilon\mu}}\left[1 + \frac{4}{\pi}\left(1 + 0.2\sqrt{\frac{C}{2B}}\right)\left(\frac{C}{2B}\right) ln\left(\frac{1}{sin\frac{\pi A}{2C}}\right) + \left(2.45 + \frac{0.2\,E}{E + 2B}\right)\left(\frac{EC}{2AB}\right)\right]^{-\frac{1}{2}} \tag{4}$$

where µ and ε are the permeability and the permittivity of the dielectric filling the waveguide, respectively. As an initial value for step thickness $\lambda_g/4$ at the central frequency of the design could be employed:

$$\lambda_g = \frac{\lambda}{\sqrt{1 - \left(\frac{\lambda}{\lambda_c}\right)^2}} \tag{5}$$

where λ_c is the cut-off wavelength. Meanwhile, the rotation angles are initially set to 30º for the first step and 60º for the second step, and the radius of the lobes is set to 0. This radius is later increased to improve the bandwidth.

The parameters A and E have a major impact on the resonance at higher frequencies. Although increasing the value of A and reducing E tends to improve the overall match of the twist, the unwanted resonance relocates inside the operational RF bandwidth. A similar effect is observed when the radius of

This article has been accepted for publication in IEEE Transactions on Terahertz Science and Technology. This is the author's version which has not been fully edited and content may change prior to final publication. Citation information: DOI 10.1109/TTHZ.2022.3213468

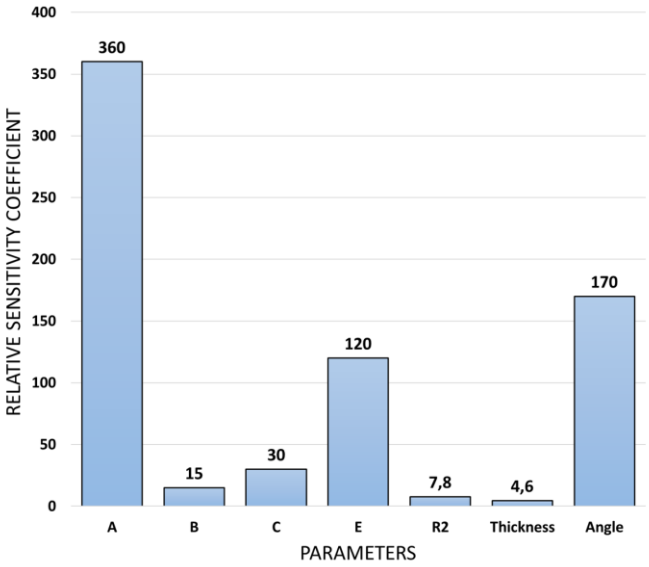

Fig. 4. Tolerance analysis using a relative sensitivity coefficient. This analysis shows that the parameters A, E, and the angle are the most sensitive.

TABLE I

Dimensions of Fabricated Twists

Parameter	Designed	Fabricated Twist T1		Fabricated Twist T2	
		Step 1	Step 2	Step 1	Step 2
A (μm)	318	315	316	335	325
B (μm)	267	270	271	287	274
C (μm)	622	630	630	628	634
E (μm)	166	165	160	146	154
R2 (μm)	85	87	84	86	93
Thickness Total (μm)	420	410		425	
Angle 1 (deg)	22.5	24.5		23.5	
Angle 2 (deg)	67.5	70.5		66.5	

the lobes is set above 85 μm. The radius R1 is introduced solely to ease the fabrication by milling and it does not affect the overall performance.

B. Sensitivity Analysis and Fabrication

Designing a twist that accomplishes a return loss level better than 20 dB over such an extremely wide frequency range represents a challenging task. Due to the high frequency at which this twist aims to operate, the fabrication alignment between the different steps could introduce variations in the performance. Therefore, the twist was fabricated using a single washer milled from both sides. This allows to fulfill the tolerance requirements, ease the fabrication and reduce the measurement uncertainties.

The overall sensitivity of the design was analyzed employing a relative sensitivity coefficient RS_{S11} [27], [28]. The coefficient is described as follows:

$$RS_{S11} = \left| \frac{\Delta S11/S11_0}{\Delta V/V_0} \right| \qquad (6)$$

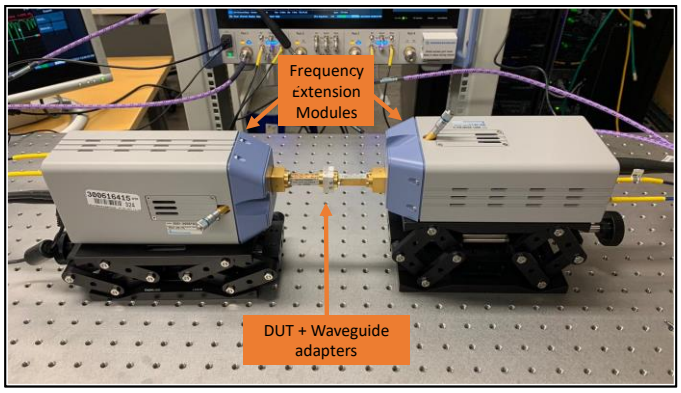

(a)

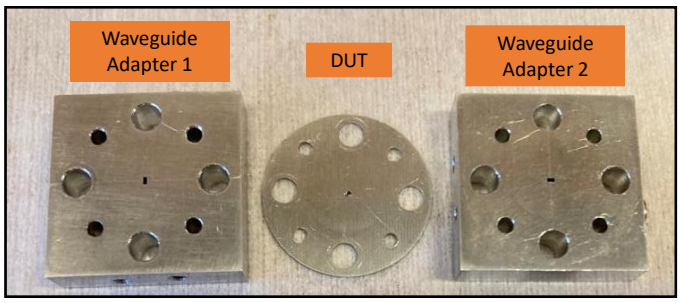

(b)

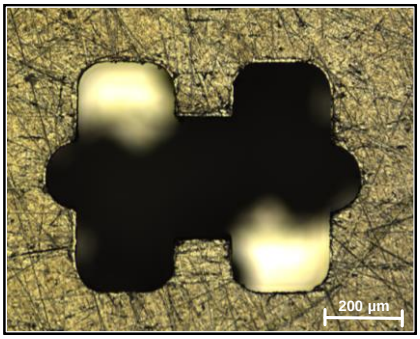

(c)

Fig. 5. (a) Measurement setup for WR 2.2 frequency extension modules. In order to perform the measurement, one of the modules is rotated 90°. (b) Waveguide adapters employed for the measurement. A pair of adapters were use for each measured frequency band. The fabricated twist is depicted between the adapters. The twist incorporates a UG385/U standard flange. (c) Zoom over the the fabricated twist. The second step is seen in the background of the picture.

where $\Delta S11$ represent the variation of the S11 parameter when a small change in one of the design parameter ΔV is introduced. Meanwhile, the rest of the parameters remain fixed. V_0 and $S11_0$ denote the designed value of the parameter and the S11 response, respectively. Since the twist is a passive device, the same analysis is valid for S22 sensitivity. The relative sensitivity coefficient was evaluated at the center frequency for the different parameters. The result shown in Fig. 4 indicates that the higher the derivative value, the more sensitive is S11 with respect to that variable. From this study, it is clear that parameter A is the most sensitive, followed by E and the rotation angle. The sensitivity in A and E can be understood by considering each step of the twist as a ridge waveguide, see Fig.

This article has been accepted for publication in IEEE Transactions on Terahertz Science and Technology. This is the author's version which has not been fully edited and content may change prior to final publication. Citation information: DOI 10.1109/TTHZ.2022.3213468

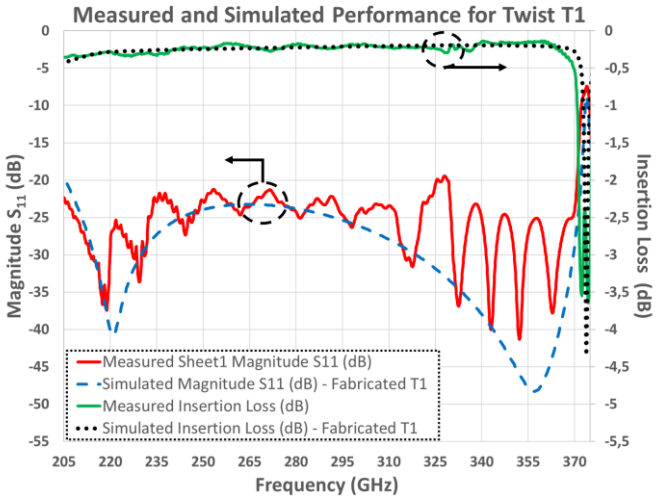

Fig. 6. Experimental results for twist T1.

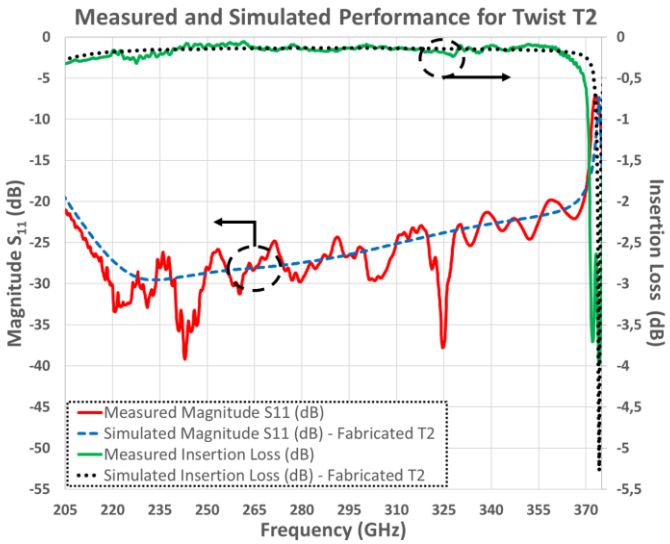

Fig. 7. Experimental results for twist T2.

1a and Table 1. As analyzed in [29], the waveguide impedance of the ridge waveguide depends on the A and E of our design. Consequently, the matching of the structure is most sensitive to these parameters too.

To assess the fabrication repeatability of the proposed design, two twists were fabricated and inspected under an optical measurement tool. Both twists were fabricated as a washer of aluminum. The parameters of the designed and fabricated twists are listed in Table 1. It is important to note that both steps of the twist were analyzed separately. From the table, it is observed that the second twist presents larger discrepancies.

III. Results and Discussion

The waveguide twists were characterized using the Rohde & Schwarz R&S® ZNA Vector Network Analyzer and frequency extension modules. Due to the considerable fractional bandwidth of the twist, three pairs of extension modules for different frequency ranges were employed in the measurements, i.e. WR-5.1 (140-220 GHz), WR3.4 (220-325 GHz), and WR2.2 (325-500 GHz). The data obtained from the different extension modules were combined to obtain the response over the whole target frequency range. In each case, a standard TRL calibration was employed. Since the proposed twist was designed for the waveguide size 800µm x 400µm, a pair of adapters was employed to accommodate the required waveguide dimension of the VNA extension modules. These adapters were later characterized and de-embedded by post-processing to obtain the frequency response of the twists. The measurement setup for the WR2.2 modules is shown in Fig.5.

TABLE II
Comparison of The State of The Art Waveguide Twists

Ref	Frequency (GHz)	Fractional Bandwidth	Total Length (λ_g)	IL* (dB)	RL** (dB)
[30]	220-320	37%	> 4	0.5	~20
	500-700	33%	-	2.5	20
[17]	75-110	37%	1.12	0.11	25
[23]	600-750	22%	0.43	0.5	20
[31]	220-330	40%	8.75	0.6	~25
[22]	140-220	44%	0.3	0.4	~20
[21]	220-330	40%	18.14	1	25
This Work	**205-365**	**56%**	**0.3**	**0.3**	~20

*IL: Insertion Loss **RL: Reflection Loss

A comparison between the simulated and measured performance of the two fabricated twists is illustrated in Fig. 6 and 7 In both cases, the return loss is better than 20 dB over most of the band, whereas insertion losses are below 0.3 dB. From the measurements, it is seen that the resonance initially outside the frequency band moved to lower frequencies. To understand the shift of the performance towards lower frequencies, the measured sizes presented in Table 1 were introduced into the simulations. These simulations accurately predict the behavior of both fabricated twists, as depicted in Fig. 6 and 7. Interestingly, T1 presents a response closer to the designed twist. This could be explained by a higher accuracy in the fabrication as illustrated in Table 1. In particular, T1 shows a higher precision in some of the most sensitive parameters, i.e. A and E. It is important to note that despite the mechanical deviations in fabrication both twists reach an outstanding 56% fractional bandwidth in the frequency range 205-365 GHz. This indicates that the proposed twist is rather tolerant to geometrical variations and it can be easily fabricated through simple techniques such as direct milling.

The twist proposed in this work is compared with the state-of-the-art 90° waveguide twist found in the literature in Table 2. It is seen that the proposed waveguide twist covers the larger fractional bandwidth, with the lower insertion loss and thickness. Although the designs presented in [31] and [21] achieved an excellent performance, their compactness is compromised since they are integrated into a split block, and thus, subject to misalignment and leaky split. Moreover, the devices explored in [30] and [23] include multiple sharp corners, increasing the fabrication complexity. From the comparison, it becomes clear that our proposed twist combines a highly compact design with a remarkable fractional

bandwidth and low insertion loss. Moreover, the absence of sharp corners makes the design suitable for milling techniques at least up to 375 GHz. Furthermore, the presented design can be easily scaled down to lower frequencies, extending its applicability.

III. Conclusion

A novel 90° compact twist with simple geometry has been designed, measured and fabricated. Measurements results confirmed that the return loss is better than 20 dB over the frequency range 205-365 GHz, which corresponds to a 56% fractional bandwidth. This implies that practically the proposed twist can cover the entire operational bandwidth of the waveguide, except for a small fraction where the proximity to cut-off frequency enhances the losses. We have shown that our twist is well-suited for fabrication through direct milling techniques at least up to 365 GHz with fair repeatability. The design is compact and brings ease to manufacturing since it is integrated into a single metallic washer. Moreover, its simplicity and compactness make it suitable and advantageous for a wide variety of applications from microwave to millimeter-wave ranges.

III. Acknowledgment

The authors would like to thank Robert Eskilsson for facilitating the measurement by providing lending of the equipment. Moreover, the authors wish to thank Sven-Erik Ferm and Mathias Fredrixon for the fabrication of the twist and waveguide adapters.

The research was carried out with financial support from Onsala Space Observatory.

References

[1] P. H. Siegel, “Terahertz technology,” *IEEE Trans. THz Sci. Technol.*, vol. 50, no. 3, pp. 910–928, March 2002.

[2] P. Yagoubov, T. Mroczkowski, V. Belitsky, D. Cuadrado-Calle, F. Cuttaia, G. A. Fuller, J. D. Gallego, A. Gonzalez, K. Kaneko, P. Mena, R. Molina, R. Nesti, V. Tapia, F. Villa, M. Beltrán, F. Cavaliere, J. Ceru, G. E. Chesmore, K. Coughlin, C. De Breuck, M. Fredrixon, D. George,G. Gibson, J. Golec, A. Josaitis, F. Kemper, M. Kotiranta, I. Lapkin, G. López-Fernández, G. Marconi, S. Mariotti, W. McGenn, J. McMahon,A. Murk, F. Pezzotta, N. Phillips, N. Reyes, S. Ricciardi, M. Sandri,M. Strandberg, L. Terenzi, L. Testi, B. Thomas, Y. Uzawa, D. Viganò, and N. Wadefalk, “Wideband 67-116 GHz receiver development for ALMA Band 2,” *Astron. & Astrophys.*, vol. 634, p. A46, Feb. 2020.

[3] V., Belitsky *et al.*, “Facility heterodyne receiver for the atacama pathfinder experiment telescope,” in *2007 Joint 32nd Int. Conf. on Infrared and Millimeter Waves and the 15th Int. Conf. on Terahertz Electronics*, 2007, pp. 326–328.

[4] V., Belitsky *et al.* “Alma band 5 receiver cartridge-design, performance, and commissioning,” *Astron. & Astrophys.*, vol. 611, p. A98, 2018.

[5] V., Belitsky *et al.*, “Sepia–a new single pixel receiver at the apex telescope,” *Astrono. & astrophys.*, vol. 612, p. A23, 2018.

[6] A. Gong, Y. Qiu, X. Chen, Z. Zhao, L. Xia, and Y. Shao, "Biomedical applications of THz technology," *Applied Spectroscopy Reviews*, vol. 55, no 5, p. 418-438, 2020, doi:10.1080/05704928.2019.1670202.

[7] B. Ferguson and X. Zhang, "Materials for THz science and technology," *Nature Materials*, vol. 1, no 1, p. 26-33, Sep. 2002,doi: 10.1038/nmat708.

[8] H. Tataria, M. Shafi, A. F. Molisch, M. Dohler, H. Sjöland, an F. Tufvesson, “6G Wireless Systems: Vision, Requirements, Challenges, Insights, and Opportunities,” *arXiv e-prints*, p. arXiv:2008.03213, Aug. 2020.

[9] C. D. Alwis, A. Kalla, Q.-V. Pham, P. Kumar, K. Dev, W.-J. Hwang, and M. Liyanage, “Survey on 6G frontiers: Trends, applications, requirements, technologies and future research,” *IEEE Open Journal of the Communications Society*, vol. 2, pp. 836–886, 2021.

[10] J. Carpenter, D. Iono, F. Kemper and A. Wootten, (2020), "The ALMA Development Program: Roadmap to 2030," *in Monthly Newsletter of Int. URSI Commission J. Radio. Astron., Preprint*, Jan. 2020.

[11] M.C., Wiedner *et al.*, “Heterodyne Receiver for Origins,” *J.l of Astronomical Telescopes, Instrum., and Syst.*, vol. 7, no. 1, pp. 1– 24, 2021.

[12] M.C., Wiedner *et al.*, “A proposed heterodyne receiver for the origins space telescope,” *IEEE Trans. THz Sci. Technol.*, vol. 8, no. 6, pp. 558–571, 2018.

[13] I., Mehdi *et al.*, “Far-infrared heterodyne array receivers,” *Bulletin of the American Astron. Society*, vol. 51, no. 7, 2019

[14] W. H. T. Vlemmings, T. Khouri, I. Mart´ı-Vidal, D. Tafoya, A. Baudry, S. Etoka, E. M. L. Humphreys, T. J. Jones, A. Kemball, E. O’Gorman, A. F. Pérez-Sánchez, and A. M. S. Richards, “Magnetically aligned dust and SiO maser polarisation in the envelope of the red supergiant VY Canis Majoris,” *Astron. & Astrophys.* , vol. 603, p. A92, Jul. 2017.

[15] J. Doane, “Low-loss twists in oversized rectangular waveguide,” *IEEE Trans. on Microw. Theory and Techn.*, vol. 36, no. 6, pp. 1033–1042, 1988.

[16] F., Duncan *et al.*, “Review: far-infrared instrumentation and technological development for the next decade,” *J. of Astronomical Telescopes, Instrum., and Syst.*, vol. 5, no. 2, pp. 1 – 34, 2019.

[17] M. A. Al-Tarifi and D. S. Filipovic, “Design and fabrication of a full w-band multi-step waveguide 90° twist,” *IEEE Microw. Wirel. Compon. Lett.*, vol. 26, no. 11, pp. 903–905, 2016.

[18] U. Rosenberg and R. Beyer, “Compact waveguide twist design fitting with interfacing waveguide cross sections,” in *2012 IEEE/MTT-S Int. Microw. Symposium Digest*, 2012, pp. 1–3.

[19] H. Asao, G. Hiraiwa, and A. Katayama, “A compact 90-degree twist using novel ridged waveguide for integrated waveguide subsystems,” in *2006 European Microw. Conf.*, 2006, pp. 1185–1188.

[20] A. Kirilenko, D. Y. Kulik, and L. A. Rud, “Compact 90 twist formed by a double-corner-cut square waveguide section,” *IEEE Trans. Microw.*

[21] L. Zeng, C. E. Tong, S. N. Paine, and P. K. Grimes, “A compact machinable 90° waveguide twist for broadband applications,” *IEEE Trans. Microw. Theory Tech.*, vol. 68, no. 7, pp. 2515–2520, 2020.

[22] C. López, V. Desmaris, D. Meledin, A. Pavolotsky, and V. Belitsky, “Design and implementation of a compact 90° waveguide twist with machining tolerant layout,” *IEEE Microw. Wirel. Compon. Lett.*, vol. 30, no. 8, pp. 741–744, 2020.

[23] L. Chen et al., "A Micromachined Terahertz Waveguide 90° Twist," IEEE Microw. Wireless Compon. Lett., vol. 21, no. 5, pp. 234-236, May. 2011.

[24] M. A. Al-Tarifi and D. S. Filipovic, "Design and Fabrication of a Full W-Band Multi-Step Waveguide 90° Twist," in *IEEE Microw. Wirel. Compon. Lett*, vol. 26, no. 11, pp. 903-905, Nov. 2016, doi: 10.1109/LMWC.2016.2615025.

[25] J. Helszajn, "Impedance and propagation in ridge waveguides using the transverse resonance method," *in Ridge Waveguides and Passsive Microwave Components*, London, United Kingdom: The institution of Engineering and Technology, 2000, ch. 4, pp. 26–29.

[26] HFSS Ansoft, ver. 19.1.0, Ansoft Corp., Pitts- burgh, PA, USA, Tech. Rep., 2018. Retrieved from https://www.ansys.com/products/electronics/ansys-hfss.

[27] C. López, V. Desmaris, D. Meledin, A. Pavolotsky, and V. Belitsky, “Waveguide-to-substrate transition based on unilateral substrateless fin-line structure: Design, fabrication, and characterization,” *IEEE Trans. THz Sci. Technol.*, vol. 10, no. 6, pp. 668–676, 2020.

[28] D., Jayasankar *et al.*, “A 3.5-THz, ×6-harmonic, single-ended schottky diode mixer for frequency stabilization of quantum-cascade lasers,” *IEEE Trans. THz Sci. Technol.*, vol. 11, no. 6, pp. 684–694, nov 2021.

[29] T.-S. Chen, “Calculation of the parameters of ridge waveguides,” *IRE Trans. Microw. Theory and Tech.*, vol. 5, no. 1, pp. 12–17, 1957.

[30] G. Chattopadhyay, J. S. Ward, N. Llombert, and K. B. Cooper, “Submillimeter-wave 90° polarization twists for integrated waveguide circuits,” *IEEE Microw. Wirel. Compon. Lett.*, vol. 20, no. 11, pp. 592–594, 2010.

[31] J.-Q. Ding, Y. Zhao, and S.-C. Shi, “A full wr-3 band and low-loss 90° waveguide twist based on cnc,” *IEEE Trans. THz Sci. Technol.*, vol. 10, no. 1, pp. 93–96, 2020.

This article has been accepted for publication in IEEE Transactions on Terahertz Science and Technology. This is the author's version which has not been fully edited and content may change prior to final publication. Citation information: DOI 10.1109/TTHZ.2022.3213468

Cristian Lopez was born in Buenos Aires, Argentina, in 1990. He received the B.S. degree in electronic engineering from Facultad de Ingeniería del Ejército Grl. Div. Manuel N. Savio, Buenos Aires, Argentina, in 2012, and the M.Sc. degree in microelectronics from Universidad Politecnica de Cataluña, Barcelona, Spain, in 2018.

He is currently working toward a Ph.D. degree at Chalmers University of Technology, Gothenburg, Sweden.

His current research interests are the design and characterization of cryogenic components for THz systems.

Daniel Montofré received the double Ph.D. degree in electrical engineering from the Universidad de Chile, Santiago, Chile, and the University of Groningen, Groningen, The Netherlands, in 2020. He is a Postdoctoral Researcher with the Group for Advanced Receiver Development, Gothenburg, Sweden. His research interests focused on the development of new instruments for millimeter/submillimeter space and astronomical applications with special interest in multifrequency receivers, waveguide devices for THz detection, and optical system design.

Vincent Desmaris received the M.Sc. degree in material science from the National Institute of Applied Science, Lyon, France, in 1999, and the Ph.D. degree in electrical engineering from the Chalmers University of Technology, Gothenburg, Sweden, in 2006. His thesis concerned the fabrication, characterization, and modeling of AlGaN/GaN microwave transistors. Since 2006, he has been with the Group for Advanced Receiver Development, Chalmers University of Technology. His research interests include the area of terahertz receiver technology, especially microfabrication and characterization of waveguide components and circuits and planar cryogenic microwave devices.

Andreas Henkel received the Dipl. Ing. degree in engineering from University of Siegen in Germany in 1995. He started as support engineer in Rohde & Schwarz Engineering and Sales GmbH, covering spectrum analyzers from Advantest. He then became product manager for optical test equipment and vector network analyzers from Advantest. In 2005, he became product manager for Rohde Schwarz vector network analyzers worldwide.

Victor Belitsky (M'95–SM'07) received the M.Sc. degree in electrical engineering from the Moscow Telecommunication Institute, Moscow, Russia, in 1977, and the Ph.D. degree in experimental physics from the Institute of Radio Engineering and Electronics, U.S.S.R. Academy of Sciences, Moscow, Russia, in 1990. He is currently Professor and Head of the Group for Advanced Receiver Development, Department of Space, Earth, and Environmental Sciences, Chalmers University of Technology, Gothenburg, Sweden. His research interests include terahertz and superconducting electronics and components, instrumentation for radio astronomy, and environmental science.